

# Asymptotic structure of steady nonlinear reaction-diffusion-Marangoni convection fronts

L. Rongy,<sup>1</sup> A. De Wit,<sup>1</sup> and G. M. Homsy<sup>2</sup>

<sup>1</sup>*Nonlinear Physical Chemistry Unit and Center for Nonlinear Phenomena and Complex Systems, Université Libre de Bruxelles (ULB), CP 231, 1050 Brussels, Belgium*

<sup>2</sup>*Department of Mechanical Engineering, University of California, Santa Barbara, California 93106, USA*

(Received 13 November 2007; accepted 20 June 2008; published online 29 July 2008)

Chemical fronts propagating in horizontal liquid layers with a free surface can induce localized steady Marangoni flow. Numerical integration of the Stokes equations coupled to a reaction-diffusion-convection equation for the concentration of the surface-active reaction product shows that the system reaches an asymptotic dynamic state characterized by a deformed front surrounded by a steady convection roll traveling at a constant speed. To understand the basic balances determining this steady dynamics, we present here an asymptotic analysis of the system based on the numerically obtained scalings at high Marangoni numbers  $M$  quantifying the interaction between reaction-diffusion processes and Marangoni convection.  $M$  is positive (negative) when the product decreases (increases) the surface tension behind the front. We obtain a semianalytical solution for the product concentration for large  $M > 0$ , showing that the key balances are between reaction, convection, and vertical (rather than axial) diffusion. For  $M < 0$ , we present evidence of a multiscale structure of the front resulting from more complex balances. © 2008 American Institute of Physics. [DOI: 10.1063/1.2956987]

## I. INTRODUCTION

Chemical fronts resulting from the interplay between diffusion and autocatalytic chemical reactions have long been studied experimentally and theoretically: Such reaction-diffusion (RD) systems are also well-known examples of pattern formation.<sup>1-4</sup> Such fronts usually propagate in gels at a constant speed and with a steady shape. However, their propagation in liquid layers can be affected by convective motions driven by density, viscosity, or surface tension gradients across the front arising from concentration and temperature changes during the chemical reaction. Actually, chemical fronts of well-known reactions such as the Belousov-Zhabotinskii (BZ) reaction or the iodate-arsenous acid reaction have long been noted to propagate with non-constant velocities in horizontal thin layers of liquid in contact with air.<sup>5-12</sup> Such reactions involve variations of the solution density and surface tension, which suggests that convection resulting from a combination between buoyancy and Marangoni effects may affect the dynamics of these systems.<sup>13-16</sup>

By using simple models where only one type of convective flow is present, theoretical and numerical approaches are essential in differentiating between the various effects coming into play and in obtaining better understanding of the complex dynamics of such coupled systems. Numerous theoretical and numerical studies have analyzed the influence of pure buoyancy-driven flows on chemical fronts propagating in horizontal solution layers, showing that buoyancy effects can lead to steady convection, deformation, and acceleration of these fronts (see, for instance, Refs. 17 and 18 and references therein). On the other hand, there are relatively fewer studies of the interaction between pure Marangoni convec-

tion and chemical reactions. Numerical integration of modified Oregonator model equations coupled to Navier-Stokes equations have been performed to understand the experimental observations of convective flows at the passage of BZ waves.<sup>19-21</sup> In addition, studies of autocatalytic reactions occurring solely at the surface of a thin layer in contact with air show that Marangoni flow can stabilize interfacial solitary wave structures generated by the chemical reaction.<sup>22-25</sup> Pereira *et al.*<sup>26,27</sup> have further studied, using the lubrication approximation, the two-variable Fitzgugh-Nagumo chemical model coupled to Marangoni stresses on a thin liquid film free surface, analyzing the stability and nonlinear behavior resulting from such a coupling.

In a previous study, we numerically studied the spatiotemporal dynamics of an isothermal chemical RD front propagating in the presence of a solutal Marangoni flow in a thin horizontal layer with a nondeformable interface<sup>28,29</sup> (see Fig. 1). The reaction takes place in the bulk and produces a surface-active species while the solution density is assumed constant. One of the reaction products is surface active so that it triggers a surface tension gradient across the front, which induces a Marangoni flow deforming and accelerating the front. This interaction between RD processes and convection is quantified by a solutal Marangoni number  $M$  defined and discussed in more detail below. Our sign convention is such that when  $M > 0$ , the reaction product decreases the surface tension behind the front so that the flow induced at the surface toward the largest surface tension region, in this case the reactants, is parallel to the propagation speed of the chemical front invading those reactants. On the other hand, the surface flow is antiparallel to the front propagation direction when  $M < 0$ .

In both cases, as the flow is incompressible and occurs in

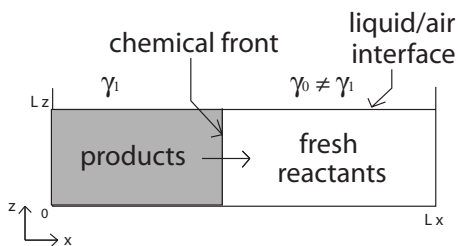


FIG. 1. Schematic of the system.

a bounded geometry, a bulk motion, or so-called “return flow,” is induced in the opposite direction to the surface flow. This flow induces a distortion of the chemical front within the layer, with the deformation zone initially increasing in time. The system next reaches an asymptotic dynamic state characterized by a deformed chemical front with constant shape and a localized and steady convection roll traveling at a constant speed with this front. Increasing the value of the Marangoni number<sup>28</sup> or the layer thickness<sup>29</sup> results in an increased deformation of the front, with the propagation speed of the steady regime and the fluid velocity being increasing functions of the absolute value of  $M$ . However there is an asymmetry between the results obtained for positive and negative  $M$ , with the flow structure becoming more complicated for large negative  $M$ . Even so, independently of the flow direction at the surface, the front always propagates at a constant speed and this propagation speed scales as  $M^{1/2}$  for large  $M$ .

The main objective of this paper is to gain further insight into the basic physical balances determining the attainment of a constant propagation speed and steady dynamics at large  $M$ . In particular, we show that a simplified equation for the concentration of the surface-active product, based on a rescaling and a semianalytical solution for the flow field, can be derived for positive  $M$ . This equation reveals that the asymptotic regime with constant wave speed propagation results from a balance between three effects: The Marangoni convection, the chemical reaction, and the vertical diffusion rather than axial diffusion. For negative  $M$ , the rescaling fails to capture the essential physical balances: The flow and concentration fields are more complex, resulting in a multiscale structure of the front at high  $M$ .

Section II introduces the mathematical formulation of the problem and reiterates the numerical observations and scalings obtained for positive and negative  $M$ . In Sec. III, we present the results of the asymptotic analysis at large positive Marangoni numbers. Section IV concerns the analysis of large negative  $M$  dynamics, and Sec. V concludes the paper with a short summary of the main findings.

## II. BASIC EQUATIONS AND NUMERICAL OBSERVATIONS

### A. Problem formulation and basic equations

Figure 1 shows the schematic representation of the problem. A miscible mixture is contained within a two-dimensional (2D) domain. Initially an isothermal sharp RD front separates reacted from unreacted fluid and propagates

along the  $x$  direction. The reaction produces a surface-active species so that the surface tension of the products  $\gamma_1$  differs from that of the reactants  $\gamma_0$ . In order to focus on Marangoni effects, the solution density is assumed constant and the surface is assumed to be nondeformable. The assumption of nondeformability is a common one and rests on the fact that a suitably defined capillary number is small so that surface tension dominates over pressure and normal viscous stress effects. We comment further on this assumption in Sec. V. We consider a low Reynolds number fluid with a finite Péclet number so that the dimensionless equations of this 2D RD-convection system are obtained by coupling the incompressible Stokes equations to a conservation equation for the surface-active product concentration  $c$ ,

$$\frac{\partial c}{\partial t} + \underline{v} \cdot \nabla c = \nabla^2 c + f(c), \quad (1)$$

$$\nabla p = \nabla^2 \underline{v}, \quad (2)$$

$$\text{div } \underline{v} = 0. \quad (3)$$

Here  $\underline{v} = (u, w)$  is the 2D fluid velocity vector and  $p$  denotes the pressure. The chemical production term  $f(c)$  is a simple one-variable monostable kinetic expression given by  $f(c) = c^2(1 - c)$ . We chose this kinetic expression because it is one of the simplest that is capable of sustaining traveling fronts between two different states when coupled to diffusion and in the absence of convection. Furthermore, it provides a good description of autocatalytic chemical systems such as the iodate-arsenous acid redox reaction.<sup>1,6</sup> As will be seen in the ensuing analysis, we expect that most, if not all, of our conclusions will be robust with respect to the choice of kinetic expression. The basic balances that are established between convection, diffusion, and reaction for positive and negative  $M$  do not depend sensitively on the exact form of  $f(c)$ : All that is necessary is that there be a finite steady speed of propagation of a chemical wave without change of form in the absence of convection.

The equations have been made dimensionless using the characteristic scales of the RD system: For time,  $\tau_c = 1/ka_0^2$ , for length,  $L_c = \sqrt{D\tau_c}$ , for velocity,  $U_c = \sqrt{D/\tau_c}$ , and for pressure,  $p_c = \mu/\tau_c$ , with  $k$  as the rate constant of the autocatalytic reaction,  $a_0$  as the initial reactant concentration,  $D$  as the molecular diffusion coefficient of the product, and  $\mu$  as the fluid viscosity (for further details see Ref. 28).

The initial condition corresponds to a planar RD front propagating in the absence of any fluid flow. Hence, the initial fluid velocity and hydrostatic pressure gradient are equal to zero and the initial condition for the surface-active product concentration is the convectionless RD profile, given by the analytical solution<sup>1,6</sup>

$$c(x, t) = \frac{1}{1 + e^{(x-vt)/\sqrt{2}}} = \frac{1}{2} \left[ 1 + \tanh\left(-\frac{\sqrt{2}}{4}(x - vt)\right) \right], \quad (4)$$

where  $v = \sqrt{2}/2$  is the constant dimensionless speed of the front in the absence of flow.

The system has rigid sidewalls, a rigid bottom, and a free upper surface. At each boundary of this domain we require

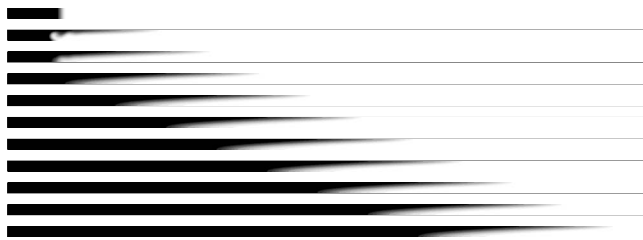


FIG. 2. Propagation of a chemical front in the presence of chemically induced Marangoni convection for  $M=500$ , shown from top to bottom from  $t=0$  up to  $t=50$  with a time interval of  $\Delta t=5$ . The aspect ratio between  $L_x=600$  and  $L_z=10$  is preserved.

zero-flux boundary conditions for the chemical concentration  $c$ . The hydrodynamic boundary conditions at the rigid boundaries are no-slip conditions  $u=0$  and  $w=0$ . At the free surface we require  $w=0$  and we use a Marangoni boundary condition for the horizontal fluid velocity  $u$  to include the changes in surface tension induced by the concentration gradient of the surface-active product along the interface. Thus,

$$x=0, \quad x=L_x, \quad \frac{\partial c}{\partial x} = u = w = 0, \quad (5)$$

$$z=0, \quad \frac{\partial c}{\partial z} = u = w = 0, \quad (6)$$

$$z=L_z, \quad \frac{\partial c}{\partial z} = w = 0, \quad (7)$$

$$\frac{\partial u}{\partial z} = -M \frac{\partial c}{\partial x}. \quad (8)$$

The last boundary condition expresses the balance of tangential stresses and, of course, is the only way in which the velocity and concentration fields are coupled. Here  $M$ , the solutal Marangoni number, is defined as

$$M = \frac{-1}{\mu \sqrt{Dk}} \frac{d\gamma}{dc}, \quad (9)$$

where  $d\gamma/dc$  is the coefficient of surface tension, assumed to be constant.

The Marangoni number quantifies the intensity of the coupling between RD processes and hydrodynamics. It is positive if the surface-active product decreases the surface tension behind the front and negative otherwise. When  $M=0$ , the surface tension is not affected by the chemical reaction so that no convective motion is present. The solution of Eqs. (1)–(3) is then a planar RD wave propagating at a constant RD speed  $v$  and with a constant shape [see Eq. (4)] in the absence of flow. When  $M \neq 0$ , convection is initiated in the solution due to the surface tension gradient across the front, which in turn results in a deformation of the planar front. The dynamics of the system is determined by an intricate interaction between reaction, diffusion, and Marangoni convection.

## B. Numerical observations

The numerical integration of Eqs. (1)–(3) with boundary conditions (5)–(8) performed in a previous study<sup>28</sup> shows that, for both positive and negative  $M$ , the system reaches an asymptotic state characterized by a vertically deformed front propagating at a constant speed and surrounded by a localized steady velocity field. The evolution to this steady state is illustrated in Fig. 2, for positive  $M=500$  and  $L_z=10$ , using 2D density plots of the product concentration ranging from  $c=0$  (white) to  $c=1$  (black) at various times. The front is first accelerated at the surface and deformed across the layer. The horizontal extent of the deformed zone first increases and then saturates to a constant while the transient velocity field evolves to an asymptotic convection roll surrounding the deformed front. The RD-convection structure shown in Fig. 3(a) propagates at a constant speed and remains steady in the comoving frame. The same kind of solution also develops for

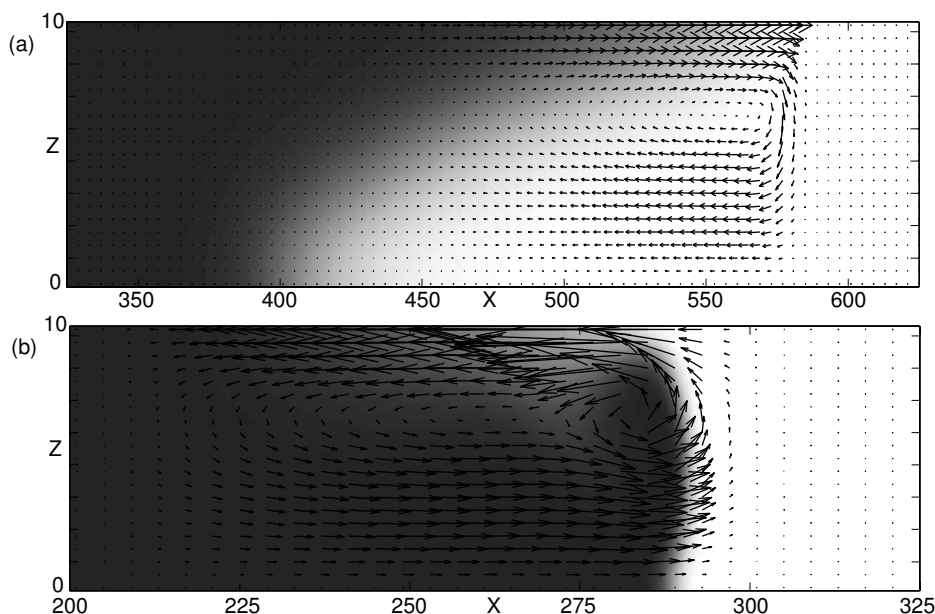


FIG. 3. Focus on the asymptotic convection roll traveling with the deformed front for  $M=500$  (a) and  $M=-500$  (b). The  $z$  direction has been magnified in order to see the details of the velocity field ( $L_z=10$ ), but the velocity vectors are displayed at the same scale in both plots.

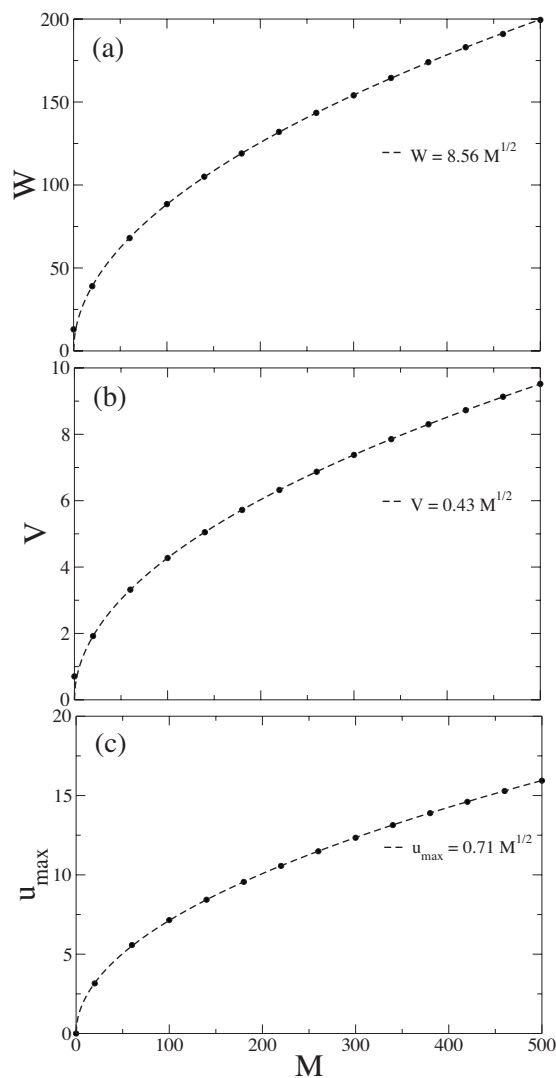


FIG. 4. Asymptotic mixing length  $W$  (a), nonlinear propagation speed  $V$  (b), and maximum horizontal fluid velocity  $u_{\max}$  (c) as a function of positive Marangoni numbers for  $L_z=10$ . The broken lines represent square root fits to the numerical data shown as filled circles.

negative  $M$  but, as shown in Fig. 3(b) for  $M=-500$ , the structure of the concentration and velocity fields is more complex with an inner vortex around an additional deformation of the concentration field.

A parametric study for  $L_z=10$  shows that the front deformation (characterized by the mixing length  $W$  defined as the distance between the tip and the rear of the concentration profile averaged along the  $z$  direction<sup>28</sup>), the propagation speed  $V$ , and the maximum horizontal fluid velocity  $u_{\max}$  all increase with  $M$ , but with important differences for  $M \leq 0$ . For  $M > 0$ , they increase as  $M^{1/2}$  for large  $M$ , as shown in Fig. 4. Figure 5 shows the same properties for negative Marangoni numbers. Since the maximum  $u$  is located at the surface for both positive and negative  $M$ ,  $u_{\max}$  is positive for  $M > 0$  and negative for  $M < 0$ . Therefore, Fig. 5(c) represents  $-u_{\max}$  as a function of  $-M$ . In the case of  $M < 0$ , we had to consider much larger values of  $|M|$  to determine the asymptotic scaling of these properties.  $W$  and  $V$  still increase as  $M^{1/2}$  while  $u_{\max}$  is a linear function of  $M$ . Besides this

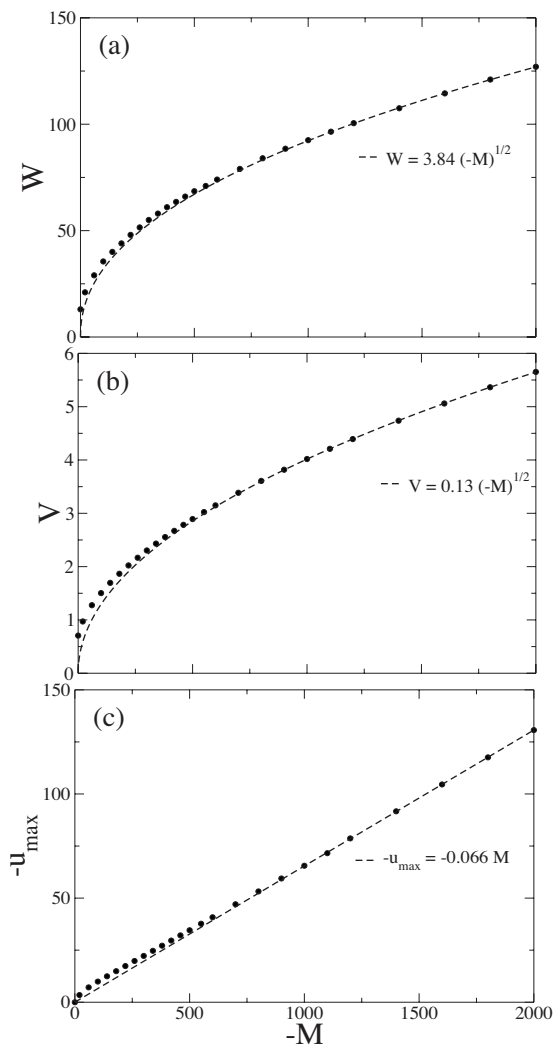


FIG. 5. Asymptotic mixing length  $W$  (a), nonlinear propagation speed  $V$  (b), and maximum horizontal fluid velocity  $-u_{\max}$  (c) as a function of negative Marangoni numbers for  $L_z=10$ . The broken lines represent power law fits to the numerical data shown as filled circles.

difference in the scalings, there is an asymmetry in the results between positive and negative  $M$ . Indeed, for the same measure of the coupling between convection and RD processes (same  $|M|$ ), the front deformation and propagation speed are larger for positive  $M$  than for negative  $M$  while the reverse is true for the maximum fluid velocity. This difference comes from the fact that the flow induced at the surface is parallel to the direction of front propagation for  $M > 0$ , while it opposes the front propagation for  $M < 0$ . Consequently, different detailed balances come into play in each case to determine the system dynamics and the constant propagating structure. In Secs. III and IV, we use the numerically determined scalings to obtain a better understanding of the physical balances involved for positive and negative  $M$ .

Finally, we comment that although these numerical results and asymptotic scalings have been obtained for a monostable autocatalytic cubic kinetics  $f(c)=c^2(1-c)$ , we have checked that they are also valid for monostable kinetics with different orders of autocatalysis, i.e., for  $f(c)=c^n(1-c)$ ,

where  $n$  is a positive integer. In particular, the case  $n=1$  is similar to the cases with  $n>1$  in contrast to buoyancy-driven flows around chemical fronts.<sup>30</sup>

### III. ASYMPTOTIC ANALYSIS: $M>0$

In this section, we rescale the equations and boundary conditions using the numerically determined scalings, which allows us to derive a simplified version of Eqs. (1)–(3) valid in the limit of  $M \rightarrow \infty$ . First of all, we eliminate the pressure gradient term by introducing the streamfunction  $\psi$  defined as

$$u = \frac{\partial \psi}{\partial z}, \quad w = -\frac{\partial \psi}{\partial x}, \quad (10)$$

and the incompressible Stokes equation is hence rewritten as a biharmonic equation for the streamfunction  $\psi$ ,

$$\nabla^4 \psi = 0. \quad (11)$$

The numerical scalings displayed in Fig. 4 show that the horizontal velocity  $u$  and the deformation of the front  $W$ , characterizing the horizontal extent of the asymptotic structure, both increase like  $M^{1/2}$ , which means that the derivatives along  $x$ ,  $\partial/\partial x$ , decrease like  $M^{-1/2}$ . Therefore, we rescale  $u$  and  $x$  with  $M^{1/2}$ , while  $w$ ,  $z$ , and  $c$  remain  $O(1)$  in order to be consistent with the continuity equation [Eq. (3)] and the Marangoni boundary condition (8). This gives the following rescaled variables:

$$u' = \frac{u}{\sqrt{M}}, \quad w' = w, \quad \psi' = \frac{\psi}{\sqrt{M}}, \quad (12)$$

$$x' = \frac{x}{\sqrt{M}}, \quad z' = z, \quad c' = c. \quad (13)$$

In this new scaling, the equation for the product concentration and the biharmonic equation become, dropping the primes,

$$\frac{\partial c}{\partial t} + u \frac{\partial c}{\partial x} + w \frac{\partial c}{\partial z} = \frac{1}{M} \frac{\partial^2 c}{\partial x^2} + \frac{\partial^2 c}{\partial z^2} + f(c), \quad (14)$$

$$\frac{1}{M^2} \frac{\partial^4 \psi}{\partial x^4} + \frac{2}{M} \frac{\partial^4 \psi}{\partial x^2 \partial z^2} + \frac{\partial^4 \psi}{\partial z^4} = 0. \quad (15)$$

In the limit of  $M \rightarrow \infty$  for which these scalings are valid, Eqs. (14) and (15) simplify to the following set of reduced equations:

$$\frac{\partial c}{\partial t} + u \frac{\partial c}{\partial x} + w \frac{\partial c}{\partial z} = \frac{\partial^2 c}{\partial z^2} + f(c), \quad (16)$$

$$\frac{\partial^4 \psi}{\partial z^4} = 0. \quad (17)$$

This simplified set of partial differential equations indicates that the viscous force due to vertical shear dominates the fluid mechanics while the evolution of the concentration field is determined by a balance between Marangoni convection, vertical diffusion, and reaction. (We note that these equations are identical to what would be expected from a lubrication theory-type set of scalings with the main hypotheses that the

derivatives along  $x$  are much weaker than the derivatives along  $z$ , while the vertical component of the velocity field  $w$  is much smaller than the horizontal component  $u$ .)

So far, our analysis has been based on numerically obtained scalings, but it is easy to see that there is only one possible set of scalings. Indeed, if we use a general scaling, i.e.,

$$u' = \frac{u}{M^\alpha}, \quad w' = \frac{w}{M^\beta},$$

$$x' = \frac{x}{M^\gamma}, \quad z' = \frac{z}{M^\delta}, \quad c' = c,$$

we find, by expressing the continuity equation and the Marangoni boundary condition in these rescaled variables, two general relations between the four power law exponents,

$$\alpha = 1 - \gamma + \delta, \quad (18)$$

$$\beta = 1 - 2\gamma + 2\delta, \quad (19)$$

which show that we cannot fix  $\alpha$  and  $\beta$  independently. Expressing the RD-convection equation in the rescaled variables, we obtain

$$M^{\alpha-\gamma} u' \frac{\partial c}{\partial x'} + M^{\beta-\delta} w' \frac{\partial c}{\partial z'} = \frac{1}{M^{2\gamma}} \frac{\partial^2 c}{\partial x'^2} + \frac{1}{M^{2\delta}} \frac{\partial^2 c}{\partial z'^2} + f(c). \quad (20)$$

As we know that the chemical reaction term  $f(c)$ , of order 1, is driving the localized and steady Marangoni flow, we can assume all the other terms in Eq. (20) to be at most  $O(1)$  and that at least one of them has to be of that order to balance the chemical reaction term. We first note that the two convective terms are of the same order and that the diffusion term along  $x$  is of lower order than the convective terms [ $\alpha - \gamma = 1 - 2\gamma + \delta > -2\gamma$  since  $\delta \geq 0$  to avoid the diffusion along  $z$  to be of larger order than  $f(c)$ ]. Hence, only three different balances for achieving a steady propagation wave are left to consider: (i) Convection balances reaction, which would give a hyperbolic equation leading to shocks and no steady propagation; (ii) vertical diffusion balances reaction, which would give no propagation along  $x$ ; and (iii) vertical diffusion and convection both balance the reaction, which implies that  $\alpha = \gamma$  and  $\delta = 0$ . Substituting this into Eqs. (18) and (19) gives the numerically observed scalings  $\alpha = \frac{1}{2} = \gamma$  and  $\beta = 0 = \delta$ .

The solution of Eq. (17) is subject to the following rescaled boundary conditions along  $z$ :

$$z = 0, \quad \psi = 0 = \frac{\partial \psi}{\partial z}, \quad (21)$$

$$z = L_z, \quad \psi = 0, \quad (22)$$

$$\frac{\partial^2 \psi}{\partial z^2} = -\frac{dc_s}{dx}, \quad (23)$$

where  $c_s = c(x, z = L_z)$  is the surface concentration of the reaction product. Simple integration of Eq. (17) gives the semi-analytical expression for the streamfunction,

$$\psi = \frac{L_z^2}{4} \frac{dc_S}{dx} z^2 (-z+1), \quad (24)$$

where the vertical coordinate  $z$  has been rescaled by the layer thickness  $L_z$  to vary between 0 and 1. The horizontal and vertical components of the fluid velocity are therefore given by

$$u = \frac{L_z}{2} \frac{dc_S}{dx} \left( -\frac{3}{2} z^2 + z \right), \quad (25)$$

$$w = \frac{L_z^2}{4} \frac{d^2c_S}{dx^2} (z^3 - z^2), \quad (26)$$

which provides expressions for the return flow observed in Fig. 3(a). This velocity field corresponds to a quasiparallel return flow with an amplitude depending on the streamwise coordinate. These results combine to give a single equation for the surface-active product concentration

$$\begin{aligned} \frac{\partial c}{\partial t} + \frac{L_z}{2} \frac{dc_S}{dx} \left( -\frac{3}{2} z^2 + z \right) \frac{\partial c}{\partial x} + \frac{L_z}{4} \frac{d^2c_S}{dx^2} (z^3 - z^2) \frac{\partial c}{\partial z} \\ = \frac{1}{L_z^2} \frac{\partial^2 c}{\partial z^2} + f(c). \end{aligned} \quad (27)$$

This equation describes the system dynamics in the asymptotic regime when the RD-convection structure is propagating at a constant speed  $V$ . This constant propagation speed is also proportional to the square root of the Marangoni number [see Fig. 4(b)] so that we can rewrite Eq. (27) in the comoving frame  $\hat{x} = x - \lambda t$ , moving at the constant rescaled propagation speed  $\lambda = V/\sqrt{M}$ . Dropping the hat, we have

$$\begin{aligned} -\lambda \frac{\partial c}{\partial x} + \frac{L_z}{2} \frac{dc_S}{dx} \left( -\frac{3}{2} z^2 + z \right) \frac{\partial c}{\partial x} + \frac{L_z}{4} \frac{d^2c_S}{dx^2} (z^3 - z^2) \frac{\partial c}{\partial z} \\ = \frac{1}{L_z^2} \frac{\partial^2 c}{\partial z^2} + f(c). \end{aligned} \quad (28)$$

This one-parameter equation gives great insight into the important balances that determine the asymptotic regime and the constant speed of propagation at large  $M$ . It shows that the front speed and structure result from a balance between three effects: The Marangoni convection, the chemical reaction, and vertical (rather than axial) diffusion. The chemical reaction generates a concentration gradient. At the surface, this gradient induces the Marangoni flow, which in turn starts to advect the concentration profile in the horizontal direction, increasing  $c$  when  $u$  is positive and decreasing it when  $u$  is negative [cf. Fig. 3(a)]. This sets up both a vertical velocity as required for mass conservation and a vertical gradient on which vertical diffusion starts to act, thereby limiting the horizontal extent of the front. The role of the vertical velocity is to limit the convective propagation of the concentration field, thus giving rise to a localized self-sustained structure.

To check the validity of this general picture [and rather than solve Eq. (28) as a nonlinear eigenvalue problem for  $\lambda$ ], we numerically integrated Eq. (27) for various values of  $L_z$  using a simple Euler method for time stepping and second



FIG. 6. Concentration field in the moving frame obtained by numerical integration of the simplified equation [Eq. (27)] for  $L_z=10$ . The aspect ratio between  $L_x=30$  and  $L_z$  is preserved.

order finite central differences in space. We checked the convergence with decreasing temporal and spatial step sizes and used no-flux boundary conditions for the concentration at the four boundaries of the system. The result of the numerical integration, presented in Fig. 6, shows a deformed front propagating at a constant speed with a steady mixing length. For example, for  $L_z=10$ , the steady wave speed  $\lambda$  is 0.427 and the mixing length is 8.94, which match the large  $M$  numerical results for the integration of the full equations [Eqs. (1)–(3)] shown in Fig. 4, in which the constants are 0.43 and 8.56, respectively. Moreover, the structure of the return flow given by Eqs. (25) and (26) is independent of  $L_z$  and the horizontal velocity  $u$  is zero, minimum, and maximum at  $z=0$  and  $2L_z/3$ ,  $z=L_z/3$ , and  $z=L_z$ , respectively, which has been observed in our previous numerical results.<sup>28,29</sup> We can therefore conclude that Eqs. (27) and (28) not only recover the results obtained by integration of the full model but also give insight into the important balances between autocatalysis, diffusion, and convection.

#### IV. ASYMPTOTIC ANALYSIS: $M < 0$

In this section, we analyze the behavior of the system for large negative Marangoni numbers. In this case, the reaction product increases the surface tension so that the induced surface flow is toward the region of the products, therefore opposing the front propagation. Focusing for the moment on the length of the reaction zone,  $W$ , Fig. 5(a) indicates that it grows asymptotically as  $|M|^{1/2}$ . Thus at first glance it might appear that the same asymptotic equation [Eq. (27)] would describe the  $M < 0$  case as well. However, attempts to integrate Eq. (27) for  $M < 0$  as an initial value problem failed in the following way. Starting with a relatively broad diffusive zone, the Marangoni stress drives a surface flow *opposite* to the direction of propagation of the RD system. This, together with the requirement of a reverse flow in order to conserve mass, quickly sharpens the front in the lower regions of the channel, suggesting the formation of a shocklike solution before numerical instability ensues. A crucial feature of these simulations is the nearly complete absence of vertical concentration gradients. These do not occur near the interface because of the opposition between the Marangoni and RD velocities, nor do they occur in the lower regions due to the convective sharpening of the front described above. Thus, Eq. (27) becomes a nearly hyperbolic equation and the initial value problem is apparently ill posed: The convective transport does not produce the strong vertical diffusion, embodied by the  $\partial^2 c / \partial z^2$  term, required to equilibrate with the chemistry. Thus, other scalings must be involved: Horizontal diffusion must continue to play a role as  $M \rightarrow -\infty$ .

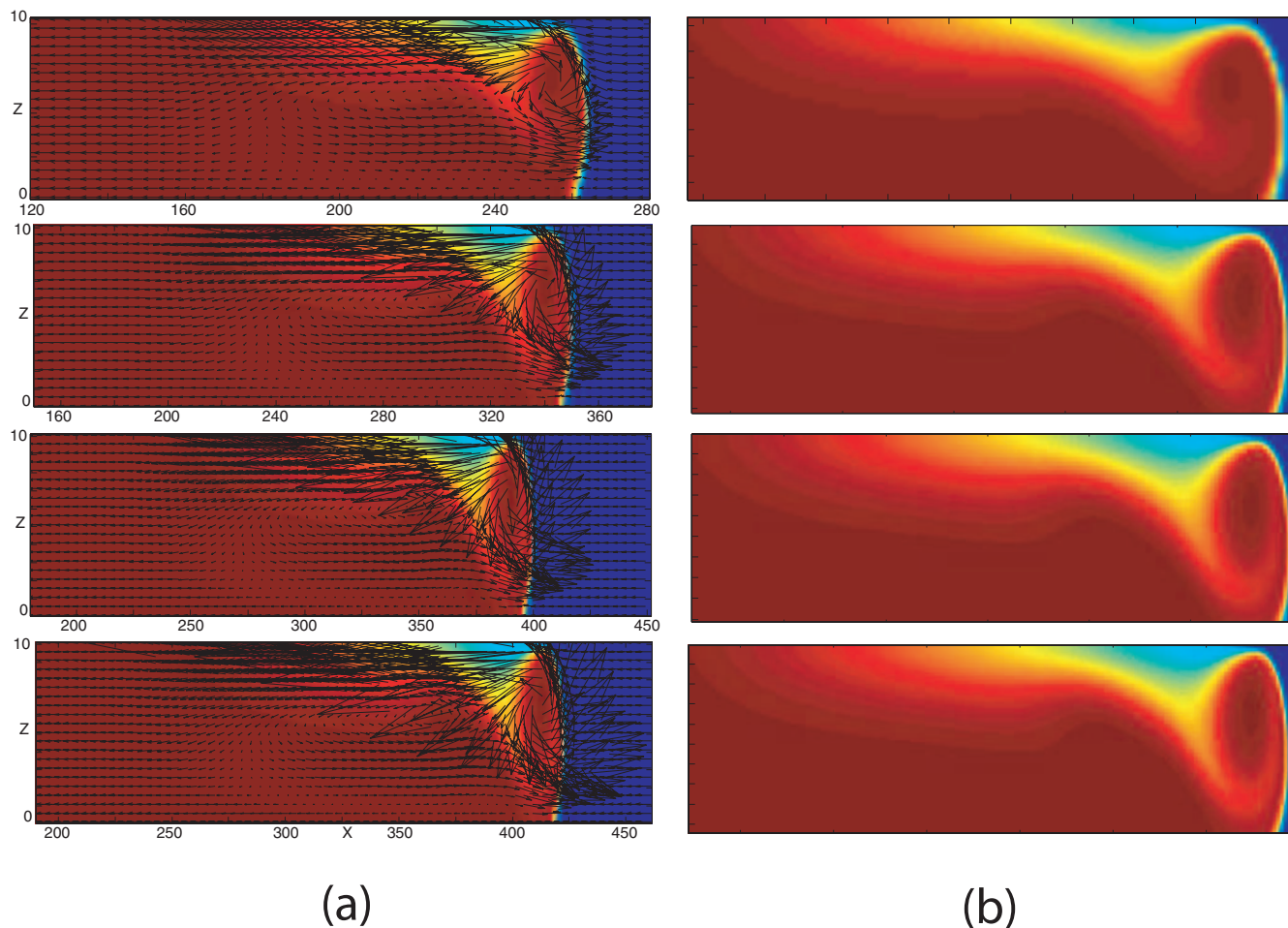


FIG. 7. (Color) (a) Asymptotic propagating structure shown in the frame moving with speed  $V$  for  $M = -1000, -2000, -2500$ , and  $-3000$ , top to bottom ( $L_z = 10$ ). The  $z$  direction has been magnified in order to see the details of the velocity field ( $L_z = 10$ ) but the velocity vectors are displayed at the same scale in the four plots. (b) Rescaled concentration fields displayed at the same size for different  $M$ . The parameters are the same as in Fig. 7(a) and the effective dimensions ( $l_x, l_z$ ) of this structure are in our dimensionless length units: (98, 8.5) for  $M = -1000$ , (135, 9.1) for  $M = -2000$ , (148.5, 9.0) for  $M = -2500$ , and (162, 9.3) for  $M = -3000$ .

The opposition between the Marangoni and RD effects lead to more complex dynamics than for positive  $M$ , but as Fig. 5 shows, the system reaches a steady dynamic state propagating at a constant speed  $V$ . Figure 7(a) shows the concentration and velocity fields for a range of large negative  $M$ . There is a convective distortion of the concentration field that increases with  $|M|$  and is accompanied by a strong inner vortex. The steady RD-convection structure is much more compact than for positive  $M$ , with a sharper reaction zone and a comparatively smaller horizontal extent [see Figs. 4(a) and 5(a) to compare the mixing length in the two cases]. This opposition also leads to the formation of a strong recirculating vortex whose intensity increases linearly with  $M$ . This can be seen in two ways.

We first examine the surface concentration gradient shown in Fig. 8 as a function of  $M$ . As can be seen, the gradient remains sharp and of the same maximum magnitude, and the horizontal distance over which the concentration gradient exists grows as  $|M|$  is increased. This large gradient produces a rapidly recirculating vortex. Second, Fig. 5(c) shows that the maximum horizontal fluid velocity  $u_{max}$ , which is located at the surface, grows as  $M^1$ . These perspectives

are consistent with one another and with the tangential stress balance [Eq. (8)]. The sharp concentration gradients seen in Figs. 7(a) and 8 cause the maximum fluid velocity  $u_{max}$  to be much greater than the front propagation speed  $V$ , opposite to the positive  $M$  case where  $V$  and  $u_{max}$  are of the

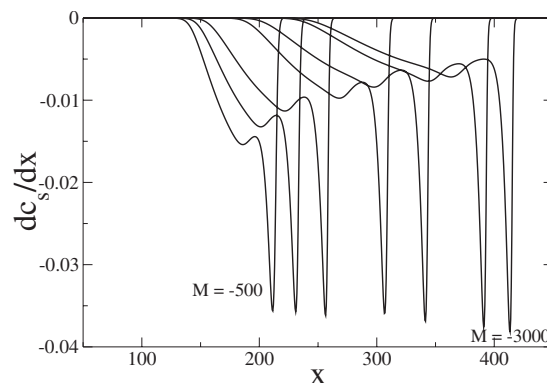


FIG. 8. Surface concentration gradient as a function of  $x$  for various Marangoni numbers,  $M = -500, -700, -1000, -1400, -2000, -2500, -3000$ , from left to right.

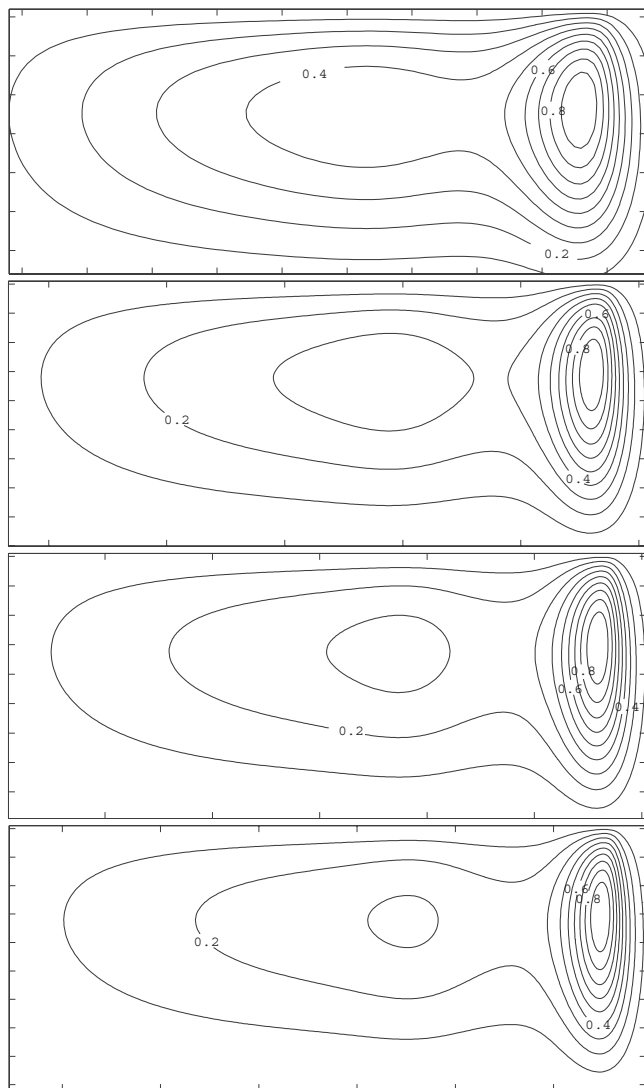


FIG. 9. Local streamfunction renormalized between 0 and 1 in the deformation zone rescaled as in Fig. 7(b) and for  $M = -1000, -2000, -2500,$  and  $-3000$ , top to bottom.

same order [compare Figs. 4(b) and 4(c) with Figs. 5(b) and 5(c)]. Moreover, two different regions in the fluid velocity field can be discerned: (i) A sharp inner collision zone involving large velocities in the recirculating vortex, and (ii) away from this region, a return flow with apparently the same structure as derived for positive  $M$ . Therefore, we can conclude that the asymptotic structure for large negative Marangoni numbers is *multiscale* and involves more complex interactions between the physical mechanisms than for positive  $M$ . The different scalings shown in Fig. 5 for large negative  $M$  confirm this observation and make analytical work more difficult.

To pursue these issues in more detail, we focus our attention on the structure of the front and search for self-similarity by examining rescalings in both  $x$  and  $z$ . The panels of Fig. 7(b) show the concentration fields in the moving frame stretched but displayed at the same heights and lengths. We determine the stretchings based on concentration

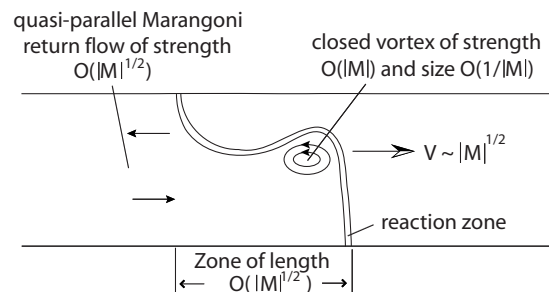


FIG. 10. Hypothesized structure as  $M \rightarrow -\infty$ .

levels: the left side and bottom are determined by the isoconcentration level  $c=0.98$ , the right side by the level  $c=0.02$ , and the surface remains the top boundary. The concentration fields appear to exhibit self-similarity when displayed in this way and the horizontal rescalings are consistent with the  $|M|^{1/2}$  scaling in Fig. 5(a). However, the same rescaling applied to the streamfunction patterns still shows some  $M$  dependence. This is illustrated in Fig. 9, showing streamline plots of  $\psi$  rescaled between 0 and 1, and reinforces our assertion that the asymptotic behavior at large negative  $M$  is a multiscale structure.

A key element is the sharpening of the concentration gradients in the lower part of the channel, which can be understood as follows: When the surface velocity and the front propagation velocity have different signs, there must necessarily be a recirculation in the lower regions of the channel with a velocity that is in the same direction as the propagation speed, with the result that convection dominates the transport of reactant until the immediate vicinity of the front. In other words, the local Péclet number is large, meaning that gradients are sharpened. The fact that the front is nearly a vertical front is due to the nearly parallel nature of the velocity field over most of the channel depth, as illustrated in Fig. 7(a).

It is difficult to make further definitive statements regarding  $M < 0$  because the asymptotic behavior in  $W$  and  $V$  develops only for  $|M| > 500$ , leaving us with approximately a decade variation in  $M$  with which to work. We will, however, end with a few speculative comments. We recall key features that distinguish the case  $M < 0$ . First, the concentration field exhibits stronger horizontal gradients due to the opposition between the RD and the Marangoni-driven flow. Second, the concentration field exhibits self-similarity when lengths are rescaled by  $|M|^{1/2}$ . This suggests the same RD-convective balance as for  $M > 0$  involving the same quasiparallel return flow. Returning to the streamfunction plots in Fig. 9, these suggest the existence of this quasiparallel flow of scale  $|M|^{1/2}$ , but superimposed on it is a recirculating vortex of strength greater than  $|M|^{1/2}$  occupying an ever more compact region near the front. These facts, taken together, lead to the hypothesized structure sketched in Fig. 10 as the asymptotic picture at infinite negative Marangoni number. Elucidation of this structure awaits further analysis.

## V. CONCLUSION

When autocatalytic chemical fronts propagate horizontally in the presence of a free surface, they can induce a localized steady Marangoni flow traveling at a constant speed with them. In the present paper, we have determined the important balances between the different physical mechanisms that result in a steady regime propagating at a constant speed, identifying that Marangoni convection, reaction, and vertical diffusion have to counterbalance each other when the direction of the surface fluid flow is parallel to the RD propagation and the resulting flow can be described uniformly by a so-called return flow ( $M > 0$ ). This description is valid for large  $M$ , i.e., when the interaction between RD processes and Marangoni convection is strong. Using the numerically obtained scalings, we have shown that the full equations can be replaced by the single simplified equation [Eq. (27)] that captures all the quantitative features of the steady regime.

In the case of negative  $M$ , the opposition between the surface flow and the front propagation leads to more complex dynamics with a strong recirculating vortex inside the main convection roll. The analysis at high  $M$  shows that the structure of the front is multiscale, which renders analytical work more difficult.

It remains to comment briefly on the range of validity of the solutions presented here. We have been concerned only with 2D solutions. Since all of our many initial value integrations of the time-dependent equations have evolved to steady solutions, we do not believe that there are any oscillatory 2D instabilities, at least over the range of parameters considered. Three-dimensional instabilities that might limit the range of applicability of the solutions are, of course, beyond the scope of the present paper. We have focused on one kinetic expression. However as already mentioned in Sec. I, the basic RD-convective balances that pertain at large Marangoni numbers are expected to be insensitive to the detailed kinetic expression used: All that is required is a steady propagating chemical reaction front in the absence of flow and Marangoni effects. Two further assumptions were made: those of low Reynolds number flow and of nondeformable interfaces. Both of these require consideration of additional physical effects and therefore additional dimensionless parameters. Inertial effects are of course measured by a Reynolds number,  $Re = U_c L_z \rho / \mu$ , and interfacial deformation by a capillary number,  $Ca = \mu U_c / \gamma$ , where in both expressions  $U_c$  is a characteristic speed. The assumptions of Stokes flow and of nondeformability are therefore most likely to break down for  $M < 0$ , where the fluid velocities are the largest. Using the dimensional scalings and the result that  $u \approx M^1$  allows one to express the local Reynolds and capillary numbers in the limit of large negative  $M$ . The expression for the capillary number becomes, under these conditions,

$$Ca \sim a_0 \frac{d\gamma/dc}{\gamma}.$$

Thus we see that the capillary number has the simple interpretation of being the fractional change in interfacial tension in going from one concentration to the other. This quantity is typically quite small but can become appreciable if the reac-

tants or products are highly surface active. While the corresponding expression for  $Re$  is not as simple, requiring it to be less than unity gives the conditions under which inertia can be neglected. Should either of these effects be non-negligible, we anticipate a modification of the asymptotic scalings developed here. Inertia will generally slow the strength of the circulation, and surface deflection will generally reduce the magnitude of the concentration gradient that remains tangent to the interface, thus reducing the Marangoni stress accordingly.

## ACKNOWLEDGMENTS

We thank A. Zebib for fruitful discussions regarding the integration of Eq. (27). L.R. is supported by a FNRS (Belgium) Ph.D. fellowship and benefited from a FNRS travel grant to visit UCSB. A.D. acknowledges financial support from Prodex (Belgium), FNRS, and from the "Communauté française de Belgique" ("Actions de Recherches Concertées" Program). G.M.H. acknowledges financial support from the National Science Foundation through Grant No. NSF/CTS-0245396.

- <sup>1</sup>A. Saul and K. Showalter, "Propagating reaction-diffusion fronts," in *Oscillations and Traveling Waves in Chemical Systems*, edited by R. J. Field and M. Burger (Wiley, New York, 1985).
- <sup>2</sup>I. R. Epstein and J. A. Pojman, *An Introduction to Nonlinear Chemical Dynamics* (Oxford University Press, Oxford, 1998).
- <sup>3</sup>J. D. Murray, *Mathematical Biology* (Springer, Berlin, 2002).
- <sup>4</sup>W. van Saarloos, "Front propagation into unstable states," *Phys. Rep.* **386**, 29 (2003).
- <sup>5</sup>T. A. Gribshaw, K. Showalter, D. L. Banville, and I. R. Epstein, "Chemical waves in the acidic iodate oxidation of arsenite," *J. Phys. Chem.* **85**, 2152 (1981).
- <sup>6</sup>A. Hanna, A. Saul, and K. Showalter, "Detailed studies of propagating fronts in the iodate oxidation of arsenous acid," *J. Am. Chem. Soc.* **104**, 3838 (1982).
- <sup>7</sup>G. Bazsa and I. R. Epstein, "Traveling waves in the nitric acid-iron (II) reaction," *J. Phys. Chem.* **89**, 3050 (1985).
- <sup>8</sup>H. Miike, H. Yamamoto, S. Kai, and S. C. Müller, "Accelerating chemical waves accompanied by traveling hydrodynamic motion and surface deformation," *Phys. Rev. E* **48**, 1627 (1993).
- <sup>9</sup>S. Kai and H. Miike, "Hydrochemical soliton due to thermocapillary instability in Belousov-Zhabotinsky reaction," *Physica A* **204**, 346 (1994).
- <sup>10</sup>S. Kai, T. Ariyoshi, S. Inanaga, and H. Miike, "Curious properties of soliton induced by Marangoni instability in shallow Belousov-Zhabotinsky reaction," *Physica D* **84**, 269 (1995).
- <sup>11</sup>O. Inomoto, T. Ariyoshi, S. Inanaga, and S. Kai, "Depth dependence of the big wave in Belousov-Zhabotinsky reaction," *J. Phys. Soc. Jpn.* **64**, 3602 (1995).
- <sup>12</sup>O. Inomoto, S. Kai, T. Ariyoshi, and S. Inanaga, "Hydrodynamical effects of chemical waves in quasi-two-dimensional solution in Belousov-Zhabotinsky reaction," *Int. J. Bifurcation Chaos Appl. Sci. Eng.* **7**, 989 (1997).
- <sup>13</sup>J. A. Pojman and I. R. Epstein, "Convective effects on chemical waves: I. Mechanisms and stability criteria," *J. Phys. Chem.* **94**, 4966 (1990).
- <sup>14</sup>K. Yoshikawa, T. Kusumi, M. Ukitsu, and S. Nakata, "Generation of periodic force with oscillating chemical reaction," *Chem. Phys. Lett.* **211**, 211 (1993).
- <sup>15</sup>O. Inomoto, K. Abe, T. Amemiya, T. Yamaguchi, and S. Kai, "Bromomalonic-acid-induced transition from trigger wave to big wave in the Belousov-Zhabotinsky reaction," *Phys. Rev. E* **61**, 5326 (2000).
- <sup>16</sup>M. J. B. Hauser and R. H. Simoyi, "Inhomogeneous precipitation patterns in a chemical wave," *Phys. Lett. A* **191**, 31 (1994).
- <sup>17</sup>D. A. Vasquez, J. M. Little, J. W. Wilder, and B. F. Edwards, "Convection in chemical waves," *Phys. Rev. E* **50**, 280 (1994).
- <sup>18</sup>L. Rongy, N. Goyal, E. Meiburg, and A. De Wit, "Buoyancy-driven convection around chemical fronts traveling in covered horizontal solution layers," *J. Chem. Phys.* **127**, 114710 (2007).

- <sup>19</sup>K. Matthiessen, H. Wilke, and S. C. Müller, "Influence of surface tension changes on hydrodynamic flow induced by traveling chemical waves," *Phys. Rev. E* **53**, 6056 (1996).
- <sup>20</sup>M. Diewald, K. Matthiessen, S. C. Müller, and H. R. Brand, "Oscillatory hydrodynamic flow due to concentration dependence of surface tension," *Phys. Rev. Lett.* **77**, 4466 (1996).
- <sup>21</sup>H. Kitahata, R. Aihara, N. Magome, and K. Yoshikawa, "Convective and periodic motion driven by a chemical wave," *J. Chem. Phys.* **116**, 5666 (2002).
- <sup>22</sup>Z. Dagan and L. M. Pismen, "Marangoni waves induced by a multistable chemical reaction on thin liquid films," *J. Colloid Interface Sci.* **99**, 215 (1984).
- <sup>23</sup>L. M. Pismen, "Composition and flow patterns due to chemo-Marangoni instability in liquid films," *J. Colloid Interface Sci.* **102**, 237 (1984).
- <sup>24</sup>Z. Dagan and C. Maldarelli, "The influence of surface tension on propagating chemo-hydrodynamic waves," *Chem. Eng. Sci.* **42**, 1259 (1987).
- <sup>25</sup>L. M. Pismen, "Interaction of reaction-diffusion fronts and Marangoni flow on the interface of a deep fluid," *Phys. Rev. Lett.* **78**, 382 (1997).
- <sup>26</sup>A. Pereira, P. M. J. Trevelyan, U. Thiele, and S. Kalliadasis, "Dynamics of a horizontal thin liquid film in the presence of reactive surfactants," *Phys. Fluids* **19**, 112102 (2007).
- <sup>27</sup>A. Pereira, P. M. J. Trevelyan, U. Thiele, and S. Kalliadasis, "Interfacial hydrodynamic waves driven by chemical reactions," *J. Eng. Math.* **59**, 207 (2007).
- <sup>28</sup>L. Rongy and A. De Wit, "Steady Marangoni flow traveling with chemical fronts," *J. Chem. Phys.* **124**, 164705 (2006).
- <sup>29</sup>L. Rongy and A. De Wit, "Marangoni flow around chemical fronts traveling in thin solution layers: Influence of the liquid depth," *J. Eng. Math.* **59**, 221 (2007).
- <sup>30</sup>D. Lima, W. van Saarloos, and A. De Wit, "Fingering dynamics of pushed vs pulled fronts," *Physica D* **218**, 158 (2006).